Composites Part C: Open Access 14 (2024) 100460

Contents lists available at ScienceDirect

Composites Part C: Open Access

journal homepage: www.elsevier.com/locate/composites-part-c-open-access

Omni first-ply-failure envelopes — A conservative approach to assess laminate failure

Erik Kappel

DLR, Institute of Lightweight Systems (SY), Lilienthalplatz 7, 38108 Braunschweig, Germany

ARTICLE INFO

Keywords:
Composite design
Laminate failure
Failure-mode concept
Optimization

ABSTRACT

Omni first-ply-failure (FPF) envelopes are an elegant yet conservative approach to assess composite laminate failure on a global level. Omni envelopes can be found increasingly in recent publications. However, the development process of those envelopes shows a lack of clarity. At some point the illustration switches from a laminate-strain basis $(\varepsilon_x, \varepsilon_y, \gamma_{xy})$ to the particular case of laminate principal-strain $(\varepsilon_I, \varepsilon_{II})$ basis. The latter is elegant, as the principal-strain space can be easily plotted in 2D. This article presents two procedures to directly determine omni FPF envelopes and it clarifies the transfer to principal strains.

While the Tsai–Wu criterion is used in almost all available publications, the present article uses Cuntze's failure mode concept (FMC). The article provides a simple example case, which demonstrates the application of omni envelopes in context of FEA based CFRP design.

1. Motivation

Well known failure criteria as Tsai–Wu [1] or Cuntze's FMC [2] usually assess ply stresses, which always require a ply-wise analysis in the local coordinate system. This is considerable effort for parts with dozens of laminate zones and hundreds of plies. The present article aims to provide a robust global laminate-failure criterion, which allows for determining laminate reserve factors. It is the ambition to use in-plane principal strain information as input for the assessment, while conventional strength parameters in stress space (X_t, X_c, Y_t, Y_c, S) remain the basis, as this is the baseline in todays certification processes. The approach offers the advantage of an easy to illustrate load state as in-plane principal strains are a standard output of today's FE tools as ABAQUS CAE [3], which is used in context of this article. The simple expression

$$\begin{bmatrix} \varepsilon_I \\ \varepsilon_{II} \\ 0 \end{bmatrix}_{laminate} = \begin{cases} \text{laminate Ok?} & \rightarrow \quad f_{RF} \geq 1. \\ \text{laminate not Ok?} & \rightarrow \quad f_{RF} < 1. \end{cases} \tag{1}$$

summarizes the ambition of the present approach, with f_{RF} denoting the reserve factor. The difficulty in context of principal laminate strains is that the principal axes are usually rotated with respect to the laminate coordinate system. The transfer from principal to laminate strains, requires transformation, which can be visualized using Mohr's circle in strain-space (see Appendix) but requires additional efforts.

The ambition of the present article is to allow an laminate assessment just based on the principal strain information, even in cases when the exact relation to the laminate coordinate system is unknown. Omni failure envelopes have been proposed in this context. Their creation and the application is demonstrated in this article.

2. First-ply-failure envelopes and omni envelopes

Omni-envelopes are created based on multiple individual failure curves of differently aligned plies, as shown in [4]. Those are all illustrated with respect to the global laminate strains ε_x, ε_y, referring to the laminate's global (x,y) coordinate system (CoS). Note, that in contrast to the majority of publications, Tsai uses the (1,2)-CoS for the laminate and the (x,y)-system for the ply's local CoS (see [1]).

Fig. 1 shows the aforementioned step from laminate strains to principal strains for Tsai–Wu (see [5, p.32]) and for Cuntze failure-mode-concept (FMC), which is in focus in the present article. Note, that the envelopes in Figs. 1(a) (left) are plotted with respect to the laminate CoS, while the right plot in Fig. 1(a) shows the envelopes referring to principal strains.

The reason for this transfer has neither been outlined nor explained in the literature. The following statement tries to summarize a personal communication with Steve Tsai, who presented FPF omni envelopes for the first time.

The idea behind the strain transfer: when all conceivable ply orientations are considered for the envelope creating, the corresponding material is isotropic. As the strain-state of an isotropic laminate/material is independent of the load introduction directions, assessing principal strain becomes

E-mail address: erik.kappel@dlr.de.

https://doi.org/10.1016/j.jcomc.2024.100460
Received 21 March 2024; Received in revised form 10 April 2024; Accepted 13 April 2024
Available online 22 April 2024

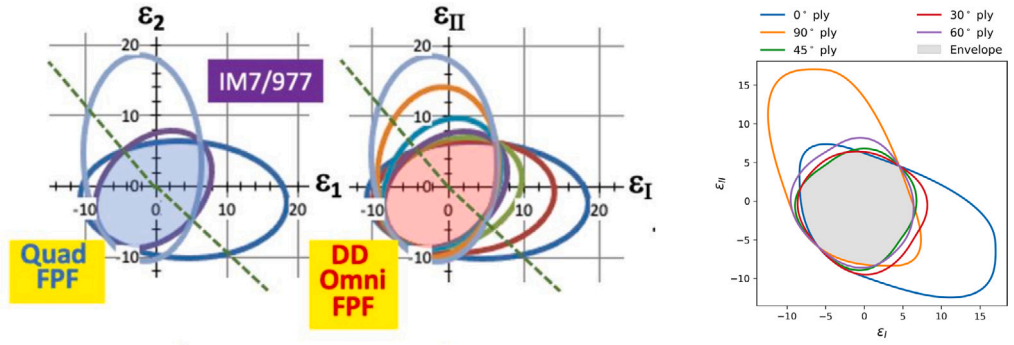

(a) Tsai-Wu envelopes (b) Cuntze2D envelope

Fig. 1. FPF for a conventional laminate (Quad) and the corresponding omni envelope. The Figure can be found in [5, p.32]. Strains in ‰. Material data in Table 1.

possible without knowing the relative rotation of the laminate CoS and the principal-axis system.

The principal strain illustration is particular interesting in context of FE simulation models. The FE code ABAQUS, for example, allows for the output of maximum and minimum in-plane principal strains. Using the 'Envelope' setting in addition, allows for plotting maxima and minima in all layers in a defined laminate, covering strain from membrane loads but also from bending.

2.1. Cuntze's FMC in 2D and material data

The ply specific effort in Cuntze's FMC [2] is determined with

$$Eff = \sqrt[m]{\left(Eff^{\parallel\sigma}\right)^m + \left(Eff^{\parallel\tau}\right)^m + \left(Eff^{\perp\sigma}\right)^m + \left(Eff^{\perp\tau}\right)^m + \left(Eff^{\perp\parallel}\right)^m} \quad (2)$$

The total effort Eff captures five mode-specific contributions. Those refer to tension ($Eff^{\parallel\sigma}$) and compression ($Eff^{\parallel\tau}$) in fiber direction, to tension ($Eff^{\perp\sigma}$) and compression ($Eff^{\perp\tau}$) in transverse direction and to shear loads ($Eff^{\perp\parallel}$). For each mode-specific effort $Eff^i = 1$ is reached when the stress reaches the corresponding strength limit.

$Eff < 1$ refers to an intact ply. $Eff > 1$ indicates the onset of failure has been passed. $Eff = 1$ refers to the ply limit. It defines the failure condition as

$$Eff = 1 = \left(Eff^{\parallel\sigma}\right)^m + \left(Eff^{\parallel\tau}\right)^m + \left(Eff^{\perp\sigma}\right)^m + \left(Eff^{\perp\tau}\right)^m + \left(Eff^{\perp\parallel}\right)^m \quad (3)$$

with the mode-specific material efforts being defined as

$$Eff^{\parallel\sigma} = \frac{\sigma_1 + |\sigma_1|}{2 \cdot X_t} \quad , \quad Eff^{\parallel\tau} = \frac{-\sigma_1 + |\sigma_1|}{2 \cdot X_c} \quad (4)$$

$$Eff^{\perp\sigma} = \frac{\sigma_2 + |\sigma_2|}{2 \cdot Y_t} \quad , \quad Eff^{\perp\tau} = \frac{-\sigma_2 + |\sigma_2|}{2 \cdot Y_c} \quad (5)$$

$$Eff^{\perp\parallel} = \frac{|\tau_{12}|}{S - \mu_{\perp\parallel} \cdot \sigma_2} \quad \leftarrow \text{!note dependency on } \sigma_2 \text{ and } \tau_{12} \quad (6)$$

The efforts Eff_i are determined from the ply stresses $[\sigma_1, \sigma_2, \tau_{12}]^T$ and five ply-strength parameters (X_t, X_c, Y_t, Y_c, S). The FMC's parameters are set to $m = 2.7$, $\mu_{\perp\parallel} = 0.2$, which is in line with previous publications and a personal recommendation of Professor Ralf Cuntze (see upcoming article [6]). The parameters m and $\mu_{\perp\parallel}$ are in general obtained based on fitting experimental data. In [7], the statement *'A good guess for isotropic and UD materials is* $\mu = 0.2$*'* is provided. In addition one finds $m = 2.7$ in the same article. As unidirectional (UD) carbon-fiber epoxy material is in focus hereafter the parameter selection is considered a reasonable selection.

The unidirectional carbon fiber/ epoxy resin prepreg IM7/977-3 material is used for the examples presented in this article. However, the presented procedures are transferable to other materials.

Table 1
Engineering constants and Strength data for IM7/977-3 UD prepreg. Constants from [1, p.321] and also in [8, p.18].

Parameter	value	unit	Parameter	value	unit
E_1	191.00	GPa	X_t	3250	MPa
E_2	9.94	GPa	X_c	1600	MPa
ν_{12}	0.35	–	Y_t	62	MPa
G_{12}	7.79	GPa	Y_c	98	MPa
			S	75	MPa

Table 1 summarizes the relevant material data, which is used for all calculations presented in this article.

In the following sections, two procedures are presented to directly determine omni envelopes. It is distinguished between the 'single-ply' and the 'all-ply' approach, as derived in the following chapters.

3. The 'single-ply' approach

Local ply stresses are determined based on global laminate strains by using (see [9])

$$\begin{bmatrix}\sigma_1\\ \sigma_2\\ \tau_{12}\end{bmatrix} = [T] \cdot [\bar{Q}] \cdot \begin{bmatrix}\varepsilon_x\\ \varepsilon_y\\ \gamma_{xy}\end{bmatrix}_{laminate} \quad . \quad (7)$$

The corresponding local stresses depend on the ply orientation (β) with respect to the global laminate CoS (x, y) (as $[T] \cdot [\bar{Q}] = f(\beta)$) and on the current laminate strain. Thus, one need to cover all conceivable ply orientations and all strain combinations, to define a conservative 'safe region' for a laminate, made from a specific material. The strain state is formulated incrementally using

$$\begin{bmatrix}\varepsilon_x\\ \varepsilon_y\\ \gamma_{xy}\end{bmatrix}_{laminate} = mag \cdot \begin{bmatrix} -1 + \frac{2}{inc-1} \cdot k & , & k \in \{0, \dots, inc-1\} \\ -1 + \frac{2}{inc-1} \cdot i & , & i \in \{0, \dots, inc-1\} \\ -1 + \frac{2}{inc-1} \cdot j & , & j \in \{0, \dots, inc-1\} \end{bmatrix} \quad , \quad (8)$$

which leads to inc^3 evaluated strain states. The mag parameter is used to adjust the total strain magnitude, which helps in the later presented limit-load identification. In the present case $mag = 0.01$ was used. The mag parameter scales the total strains to realistic magnitude ranges for the composite materials in focus, in order to receive Eff values close to 1. For the case at hand, all strain components change from -0.01 up to 0.01, in inc discrete steps. Covering positive and negative strains is essential in order to consider all conceivable load combinations. Listing 1 in the Appendix shows the corresponding Python code. With selecting $inc = 12$, 1728 strain states are examined. Increasing the number of increments is possible. However, it will lead to longer runtimes, while the envelope shapes do not change notably. Thus, $inc = 12$ is considered

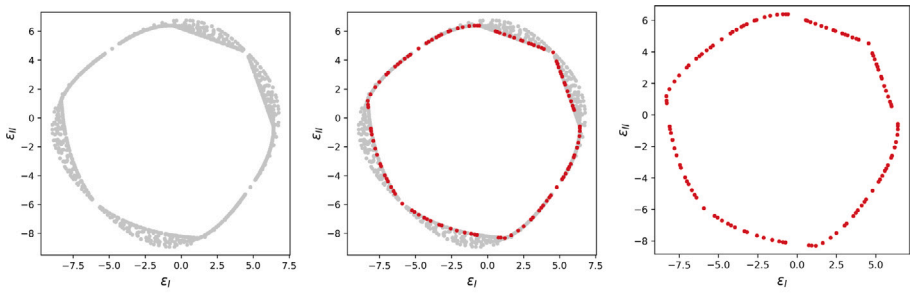

Fig. 2. Results 'single-ply' approach. Strains in ‰.

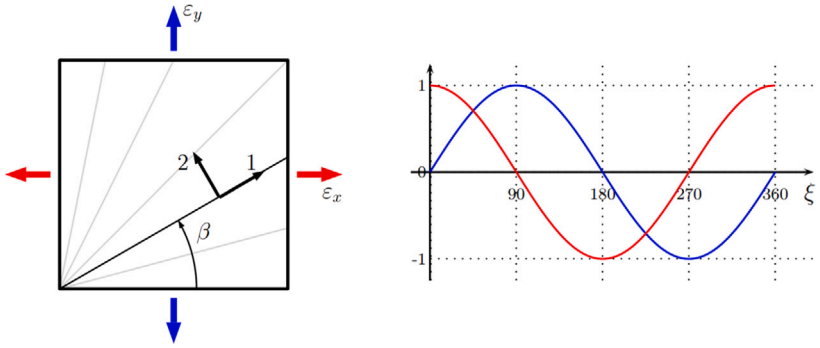

Fig. 3. FPF procedure — for each ply-orientation $0° \leq \beta \leq 90°$, 361 strain states are evaluated and the corresponding reserve factors are stored.

a reasonable choice here. Thus, the ply stresses of a ply with orientation β are calculated according to

$$\begin{bmatrix}\sigma_1\\ \sigma_2\\ \tau_{12}\end{bmatrix}_{\beta,k,i,j} = [Q]\cdot[T]_\beta^{-T}\cdot\begin{bmatrix}\varepsilon_x\\ \varepsilon_y\\ \gamma_{xy}\end{bmatrix}_{k,i,j} \quad , \tag{9}$$

with k, i, j referring to the instantaneous strain state (see). Usually, $EFF \neq 1$ is determined. Thus, the strain-state vector is scaled, using the scalar factor r_β, until $Eff = 1$ is achieved.

$$Eff\left(r_\beta\cdot\begin{bmatrix}\sigma_1\\ \sigma_2\\ \tau_{12}\end{bmatrix}_{\beta,k,i,j}\right) = 1 = Eff\left([Q]\cdot[T]_\beta^{-T}\cdot r_\beta\cdot\begin{bmatrix}\varepsilon_x\\ \varepsilon_y\\ \gamma_{xy}\end{bmatrix}_{k,i,j}\right) \tag{10}$$

This, procedure is executed for all ply orientations. For each strain-state the minimum r_β is relevant, as it refers to the most-critical ply orientation for the specific strain state.

$$r_{kij} = min\left(\left[r_{0°}, r_{1°}, \ldots., r_{90°}\right]\right) \text{ for each } (k,i,j)\text{-state} \tag{11}$$

The determined, most critical strain states determine the final envelope. For each case the corresponding principal strains are calculated using

$$\begin{bmatrix}\varepsilon_I\\ \varepsilon_{II}\\ 0\end{bmatrix}_{k,i,j} = f\left(r_{kij}\cdot\begin{bmatrix}\varepsilon_x\\ \varepsilon_y\\ \gamma_{xy}\end{bmatrix}_{k,i,j}\right) \quad . \tag{12}$$

Fig. 2(a) shows the results for all 91 ply orientations from 0° to 90° for all examined strain states. Increasing the number of increments leads to an increased point cloud density. In selected regions the envelope shape can already be anticipated. However in four regions the inner threshold needs to be identified. Further processing of the determined results shows that all shear-free strain states lead to dots on the inner envelope. Fig. 2(b) shows the corresponding results as red dots. It is concluded that examining all shear-free states directly leads to the envelope. Fig. 2(c) exclusively shows the envelope data for the shear-free load states. Increasing the number of increments, allows for increasing the envelope point density.

The preceding observation (only no-shear cases relevant) suggests an adaptation of the calculation process, which reduces computational efforts drastically. The incremental strain-state formulation from is exchanged by a harmonic approach, which is depicted in Fig. 3. It is described by the following formulation, with the ply-angle being $[0° \leq \beta \leq 90°]$ and load varying with $[0° \leq \xi \leq 360°]$. It is denoted as 'harmonic approach', as strain is modeled using sine and cosine terms.

$$\begin{bmatrix}\sigma_1\\ \sigma_2\\ \tau_{12}\end{bmatrix}_{\beta,\xi} = [T]_\beta\cdot[\bar{Q}]_\beta\cdot\begin{bmatrix}\cos\xi\\ \sin\xi\\ 0\end{bmatrix} \tag{13}$$

361 calculations for each ply orientation are executed with the fine setting for ξ. Similar, as above, each load state is scaled until $Eff = 1$ is reached. Fig. 4 shows the result of 'harmonic approach' approach. The red dots are those from Fig. 2(c), while the black solid line is determined with the harmonic approach. It can be seen that the full strain incrementation and the harmonic approach lead to identical results.

3.1. A comment on principal strains

Principal strains $\varepsilon_{I,II}$ for an arbitrary strain-state are determined using Mohr's relation (see [1, pp. 44–45])

$$\varepsilon_{I,II} = \frac{\varepsilon_x+\varepsilon_y}{2} \pm \sqrt{\left(\frac{\varepsilon_x-\varepsilon_y}{2}\right)^2 + \left(\frac{\gamma_{xy}}{2}\right)^2} \tag{14}$$

The angle

$$\delta = \frac{1}{2}\cdot tan^{-1}\left(\frac{\gamma_{xy}}{\varepsilon_x-\varepsilon_y}\right) \quad \rightarrow \quad [-45° \leq \delta \leq 45°] \tag{15}$$

describes the rotation of the principal-axis system compared to the (x, y) system. Fig. 5 visualizes the orientation of the principal axis system for a selected load case. The right upper portion of the figure shows the corresponding shear-free load state. The red line visualizes a selected

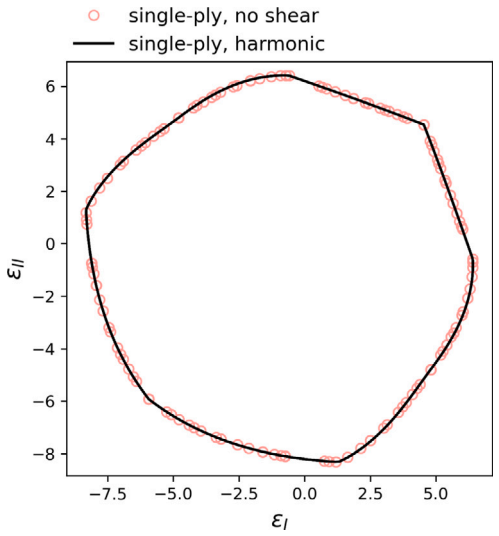

Fig. 4. Cuntze envelope from harmonic approach. The 'no shear' data refers to above's calculation procedure (see Fig. 2(c)).

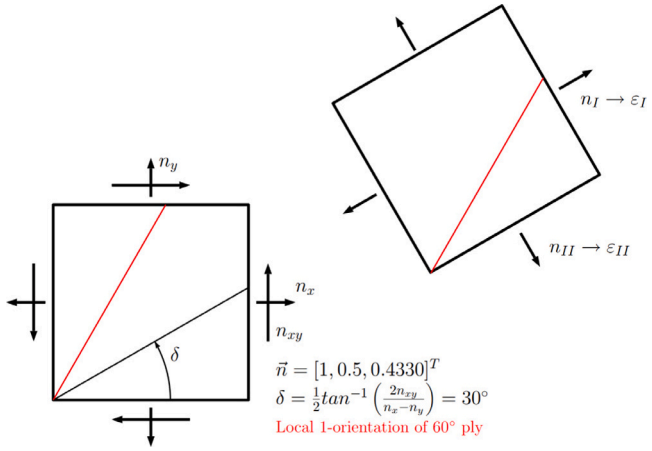

Fig. 5. Transfer from general force-loading to principal loading state. The red line shows the fiber direction of a 60° ply.

ply orientation of the laminate. When principal strain system is rotated this has no effect on the actual ply orientation.

The formulation of Eq. (13) implicitly assumes that the principal strain system is aligned with the laminate coordinate system. But, this represents a special case, only. In the general case, it would be necessary to transfer laminate strains to corresponding principal strains.

$$\begin{bmatrix} \varepsilon_I \\ \varepsilon_{II} \\ 0 \end{bmatrix} = \left([T]^{-T}\right)_\delta \begin{bmatrix} \varepsilon_x \\ \varepsilon_y \\ \gamma_{xy} \end{bmatrix} \quad . \tag{16}$$

However, the δ-rotation needs to be considered when a ply, rotated by angle β with respect to the (x, y)-system is examined. The simple case, shown in Fig. 5 shows, that the assessment of the 60° ply in the (x, y)-system is equivalent to assessing the 30° ply in the principal axis system. In the rotated principal-axis system, the effective ply angle is $\beta - \delta$. In interaction with an FE model one gets the principal strain magnitudes directly. However, the corresponding alignment of the principal axis system is no standard output parameter in FE tools. Thus, the angle δ is most often unknown, which hinders the strain transfer.

This issue can be simplified, as it is shown hereafter. When the equation for the principal axis rotation $\delta = \frac{1}{2} \cdot tan^{-1}(\ldots)$ is examined, one finds that the δ-range is limited to $[-45° \leq \delta \leq 45°]$. This information can be used, as Fig. 6 shows. The omni envelope determination process, outlined above, examines all plies in the range $[0° \leq \beta \leq 90°]$ with the strain vector $[\cos\xi, \sin\xi, 0]^T$. Fig. 6 shows, that an unknown δ leads to the fact, that in the extreme cases, with $\delta = 45°$ or $\delta = -45°$, the green illustrated orientation ranges are not covered by the examined ply-angle range. To cover those regions, the ply-angle range needs to be extended, in order to account for any possible angle δ. Thus, it is proposed to extend the examined ply-angle range to $[-45° \leq \beta \leq 135°]$. This leads to the fact, that the green-marked regions in Fig. 6 are captured. If this is realized, the harmonic strain formulation can be kept to assess all conceivable ply-orientations, independent of the relative rotation of the principal axis system. Thus, the envelope illustration in principal strains is justified.

4. The 'all-ply' laminate approach

An omni envelope circumscribes principal strains states, which can be sustained by plies oriented in all conceivable directions. In other words: a principle strain combination, which is found inside the determined *'safe region'*, will not lead to failure of a single ply in the laminate stack. The laminate stays intact. The 'single-ply' omni-envelope development process, described above, considers all conceivable ply orientations. The approach hereafter focuses on a full laminate. The laminate features ply orientations from −90° to 90°. Positive and negative angles are mandatory, to assure a balanced laminate. Thus, the laminate stacking is defined as $[-90, -89, \ldots, -1, 0, 0, 1, 2, \ldots, 89, 90]_T$, with $t_{lam} = 2 \cdot 91 \cdot 0.125$ mm $= 22.75$ mm. The corresponding in-plane stiffness matrix $[A]$ and the thickness-normalized in-plane stiffness matrix $[A^*] = [A]/t_{lam}$ are given by

$$[A] = \begin{bmatrix} 1838920.3 & 541092.4 & 0.0 \\ 541092.4 & 1838920.3 & 0.0 \\ 0.0 & 0.0 & 638659.8 \end{bmatrix} \frac{\text{N}}{\text{mm}} \quad ,$$

$$[A^*] = \begin{bmatrix} 80831.7 & 23784.3 & 0.0 \\ 23784.3 & 80831.7 & 0.0 \\ 0.0 & 0.0 & 28073.0 \end{bmatrix} \frac{\text{N}}{\text{mm}^2}$$

The 'all-ply' laminate is in-plane isotropic, as plies are aligned in all conceivable directions from −90° to 90°. For each load combination $(n_x, n_y, n_{xy})_k$ the resulting laminate strains are determined, according to

$$\begin{bmatrix} \varepsilon_x \\ \varepsilon_y \\ \gamma_{xy} \end{bmatrix}_k = [A]^{-1} \cdot \begin{bmatrix} n_x \\ n_y \\ n_{xy} \end{bmatrix}_k = \frac{1}{t_{lam}} [A^*]^{-1} \cdot \begin{bmatrix} n_x \\ n_y \\ n_{xy} \end{bmatrix}_k \tag{17}$$

The individual load states formulated incrementally, determined by the parameter inc.

$$\begin{aligned} n_{x,y,xy} &= [-1, \ldots, 1]_{inc=11} \\ &= [-1.0, -0.8, -0.6, \ldots, 0.6, 0.8, 1.0] \end{aligned} \tag{18}$$

From the load-specific resulting laminate strain, the corresponding local ply stresses of all plies in the stack are determined.

$$\begin{bmatrix} \sigma_1 \\ \sigma_2 \\ \tau_{12} \end{bmatrix}_{\beta,k} = [Q] \cdot [T]_\beta^{-T} \cdot \begin{bmatrix} \varepsilon_x \\ \varepsilon_y \\ \gamma_{xy} \end{bmatrix}_k$$

$$\text{with } [Q] = [S]^{-1} = \begin{bmatrix} 1/E_1 & -\nu_{12}/E_1 & 0 \\ -\nu_{12}/E_1 & 1/E_2 & 0 \\ 0 & 0 & 1/G_{12} \end{bmatrix}^{-1}$$

Cuntze's 2D criterion is evaluated for each ply and the ply-specific efforts

$$Eff_{\beta,k}^{(n_x,n_y,n_{xy})} = f\left(\begin{bmatrix} \sigma_1 \\ \sigma_2 \\ \tau_{12} \end{bmatrix}_{\beta,k}\right) \tag{19}$$

are stored. The ply with the highest effort is selected from all plies. The corresponding reserve factor is calculated

$$f_{RF} = \frac{1}{Eff} \tag{20}$$

The Cuntze FMC is nonlinear in the $Eff^{\perp\parallel}$ term, as it depends on τ_{12} and σ_2 and due to the exponent m. Thus, a simple scaling of the load using the reserve factor does usually not lead to fulfilling the failure condition with $Eff = 1$. Instead one gets:

$$Cuntze\left(f_{RF} \cdot \begin{bmatrix} \sigma_1 \\ \sigma_2 \\ \tau_{12} \end{bmatrix}_{\beta,k} \right) > 1 \tag{21}$$

as proportionality is not given for the

$$Eff^{\perp\parallel} = \frac{|f_{RF} \cdot \tau_{12}|}{S - \mu_{\perp\parallel} \cdot f_{RF} \cdot \sigma_2} \not\propto f_{RF} \quad . \tag{22}$$

parameter.

To circumvent this issue, a simple iterative process has been realized in the analysis code. It features multiple load-iteration steps to account for the aforementioned nonlinearity, in order to approach $Eff = 1$. Calculations show that already after three iterations $Eff = 1$ is reached with satisfying accuracy.

$$Eff_{\beta}^{(n_x,n_y,n_{xy})} = Cuntze\left(f_{RF,1} \cdot f_{RF,2} \cdot f_{RF,3} \cdot \begin{bmatrix} \sigma_1 \\ \sigma_2 \\ \tau_{12} \end{bmatrix}_{\beta,k} \right) \tag{23}$$

More advanced approaches are conceivable, but Section 5 shows that the simple approach is well suited. The limit load vector is determined to

$$\vec{n}_{max} = f_{RF,1} \cdot f_{RF,2} \cdot f_{RF,3} \cdot \begin{bmatrix} n_x \\ n_y \\ n_{xy} \end{bmatrix}_k = r_{max} \cdot \begin{bmatrix} n_x \\ n_y \\ n_{xy} \end{bmatrix}_k \quad , \tag{24}$$

which leads to a corresponding laminate strain state

$$\begin{bmatrix} \varepsilon_x \\ \varepsilon_y \\ \gamma_{xy} \end{bmatrix}_{0,max} = \frac{r_{max}}{t_{lam}} \cdot [A^*]^{-1} \cdot \begin{bmatrix} n_x \\ n_y \\ n_{xy} \end{bmatrix}_k \tag{25}$$

for each examined load case k. Eq. (14) is used again to determine the principal strains, which are the basis for plotting the omni envelope. The preceding analysis leads to the critical principal strain state for the kth load combination $(\varepsilon_I, \varepsilon_{II})_k$. It represents a single dot of the final envelope. Thus, the process is evaluated inc^3 times, similar as before in the presented 'single-ply' approach.

Fig. 7 shows the results of the described approach as green dots. The black line represents the result of the 'single-ply' approach, already shown in Fig. 4.

Similar as in the described 'single-ply' approach, the general load case can be transferred into a shear-load-free case by applying the following relations .

$$\begin{bmatrix} n_I \\ n_{II} \\ 0 \end{bmatrix} = \begin{bmatrix} c^2 & s^2 & 2sc \\ s^2 & c^2 & -2sc \\ 0 & 0 & 0 \end{bmatrix} \cdot \begin{bmatrix} n_x \\ n_y \\ n_{xy} \end{bmatrix} \quad \text{with} \quad \delta = \frac{1}{2} \arctan\left(\frac{2 \cdot n_{xy}}{n_x - n_y} \right) \quad , \tag{26}$$

with $c = \cos(\delta)$ and $s = \sin(\delta)$. The axes of the shear-load-free load state are rotated by the angle δ compared to the (x, y) systems. As principal strains of the isotropic laminate are independent from the relative position of the load coordinate system and the laminate coordinate system it is sufficient to consider only varying n_x and n_y components and keep $n_{xy} = 0$.

$$\vec{n}_{with-shear} = \begin{bmatrix} n_x \\ n_y \\ n_{xy} \end{bmatrix} \quad \rightarrow \quad \vec{n}_{without-shear} = \begin{bmatrix} n_x \\ n_y \\ 0 \end{bmatrix} = \begin{bmatrix} n_I \\ n_{II} \\ 0 \end{bmatrix} \tag{27}$$

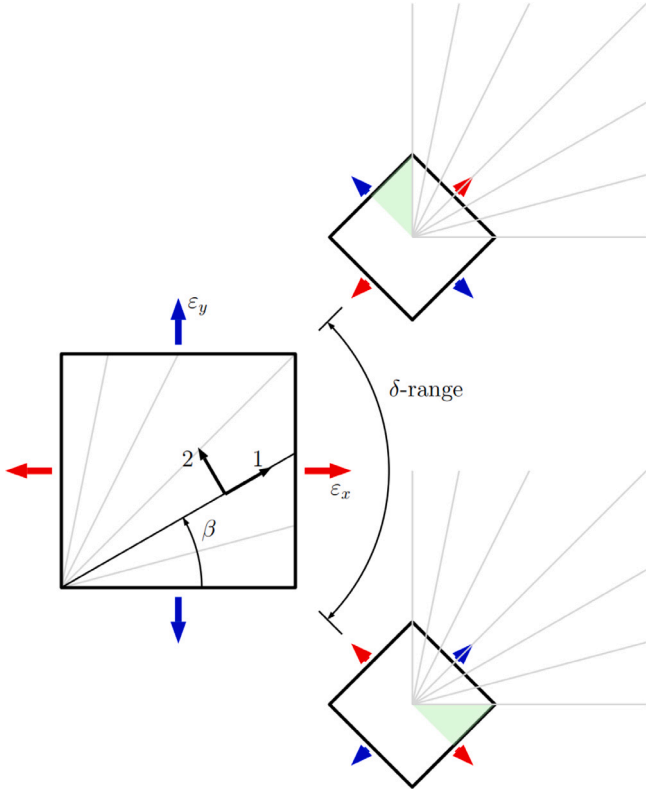

Fig. 6. Effect of principal axis rotation in context of ply-limit determinations.

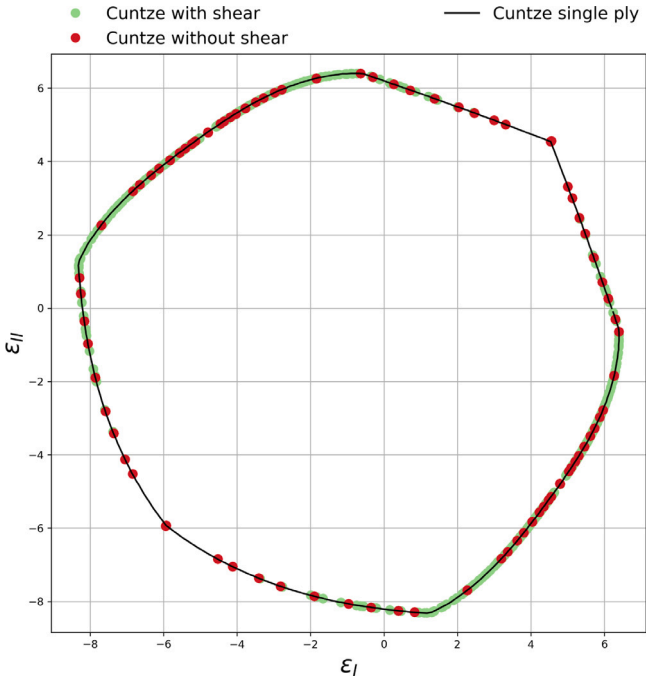

Fig. 7. Omni envelopes. Strains in ‰.

The red dots in Fig. 7 are determined following this finding. Fig. 7 summarizes the results of the 'single-ply' and the 'all-ply' approach. The plot substantiates that both approaches lead to identical results.

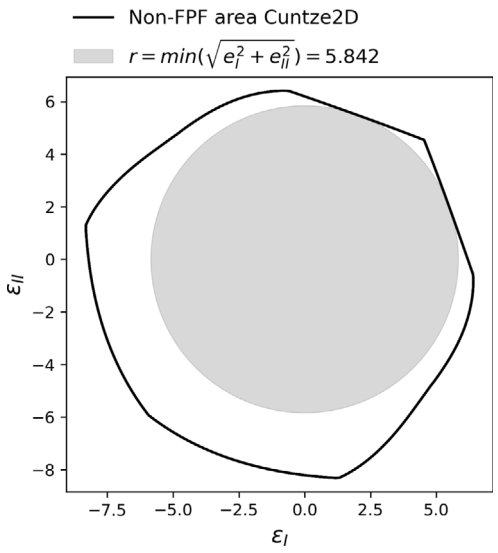

Fig. 8. Internal fitting circle. IM7/977-3.

4.1. Circle simplification

Further simplification is possible, when defining an inner fitting circle to the omni envelope (Cuntze describes it as '*Non-FPF area*' in [6]). The procedure is similar to the Unit-circle criterion, presented by Tsai and Melo [10] or its simplification, the Nettles Circle, presented in (NC) [11,12]. However, the slightly different shape of Cuntze envelopes requires a modification. The radius of an NC is determined based on the so called tensile anchors, as $r = |(\varepsilon_I, 0)|$. However, an NC would show intersection with the Cuntze envelope. Thus, the fitting-circle procedure needs to be adapted. The inner radius for a Cuntze envelope is determined based on the smallest principal-strain-vector magnitude, by using $r = min([\sqrt{\varepsilon_I^2 + \varepsilon_{II}^2}]_k)$. This procedure avoid interference between the envelope and the circle. Fig. 8 shows the inner circle, with a radius of 5.842‰.

The application of this circle in demonstrated in the following section. It is noted, that in line proposed procedures with the Nettles circle in [11], one can also define smaller radii with $r < 5.842$‰, for safety reasons e.g 3.5‰, considering an additional margin of safety.

5. Example application

A simple example case is presented in this section to demonstrate the application of omni FPF envelopes in context of FE-based CFRP design. Fig. 9 shows the schematic of the example case and its dimensions. A 50 mm long, 10 mm wide laminate is considered. Engineering constants for a unidirectional material from Table 1 are used. The modeled laminate has a quasi-isotropic layup with a $[45, -45, 90, 0]_s$ stacking sequence. A single ply is 0.25 mm thick. $\varepsilon_x = u_1/L = 0.1$ mm/50 mm = 0.2% The laminate is subjected by an asymmetric load case, which combines a linear extension in x-direction and a rotation of the right end. The resulting deformation is asymmetric as well. For the case at hand the laminates center is of interest, indicated by the red dot in Fig. 9. The omni envelope, determined above shall be used to assessment whether a certain region of the laminate can sustain the examined load case. Fig. 10 shows the corresponding FE model with illustrated boundary conditions. The initial load scenario features a 0.1 mm extension ($\varepsilon_x = u_1/L = 0.1$ mm/50 mm = 0.2%) in x-direction and a 3° end rotation, as shown in Fig. 9. The strain at the top-surface position is evaluated in the FE results.[1] The model's principal strain outputs are

$$\begin{bmatrix} \varepsilon_{max.princ} \\ \varepsilon_{min.princ} \\ 0 \end{bmatrix}_{top,center} = \begin{bmatrix} \varepsilon_I \\ \varepsilon_{II} \\ 0 \end{bmatrix} = \begin{bmatrix} 3.61965 \\ -1.44672 \\ 0 \end{bmatrix} ‰ \tag{28}$$

The corresponding absolute principal-strain-vector magnitude is determined to $\sqrt{\varepsilon_I^2 + \varepsilon_{II}^2} = 3.898$‰.

Table 2 shows the ply stresses (in local CoS) of all plies in the stack and the ply-specific total effort Eff and the mode-specific efforts (Eff_i) for the Cuntze 2D criteria.

One can see that the uppermost ply is the most critical, with a total effort of 57% ($Eff = 0.57$). Thus, the load can be increased. The comparison of the inner circle radius (5.842‰, see Fig. 8) and the current principal-strain-vector magnitude allows for determining the scaling factor to $r_{max} = \frac{5.842}{3.898} = 1.498$. Thus, displacements and rotation can be increased linearly based on r_{max}, which leads to $u_1^{LL} = 0.1498$, $u_{r2}^{LL} = 4.494°$. The corresponding principal strains change to

$$\begin{bmatrix} \varepsilon_{max.princ} \\ \varepsilon_{min.princ} \\ 0 \end{bmatrix}^{LL}_{top,center} = \begin{bmatrix} 5.42223 \\ -2.16718 \\ 0 \end{bmatrix} ‰ \tag{29}$$

which leads to the vector magnitude of $\sqrt{\varepsilon_I^2 + \varepsilon_{II}^2} = 5.839$‰. This, value represents 99.95% of the determined material-limit, which is quantified by the FPF inner fitting circle's radius. Fig. 11 shows the results. The black-edged dot represents the initial load state ($u_1 = 0.1$ mm, $ur_2 = 3°$). The red-edged circle represents the loading scaled to the circle-based limit. The corresponding ply stresses are given in Table 3.

One finds a maximum effort of 87% for the outer 45° ply. Fig. 11 visualizes the result. The red dot lies on the fitted circle circumference, but there is still a little spacing to the envelope. Iterative scaling can be used until $Eff = 1$ is reached for the first ply in the laminate. For the

Table 2
Ply stressed extracted from the FE model, corresponding efforts. From top to bottom ply.

Ply	$(\sigma_1, \sigma_2, \tau_{12})^T$ in MPa	Eff	$Eff^{\parallel\sigma}$	$Eff^{\parallel\tau}$	$Eff^{\perp\sigma}$	$Eff^{\perp\tau}$	$Eff^{\perp\parallel}$
45	$(205.07, 14.93, -39.46)^T$	0.57	0.06	0.00	0.24	0.00	0.55
−45	$(199.53, 13.18, 34.65)^T$	0.50	0.06	0.00	0.21	0.00	0.48
90	$(-186.42, 24.53, 0.31)^T$	0.40	0.00	0.12	0.40	0.00	0.00
0	$(459.43, 0.33, -0.16)^T$	0.14	0.14	0.00	0.01	0.00	0.00
0	$(382.37, 1.04, 0.00)^T$	0.12	0.12	0.00	0.02	0.00	0.00
90	$(-68.06, 14.62, -0.16)^T$	0.24	0.00	0.04	0.24	0.00	0.00
−45	$(96.02, 7.02, 10.60)^T$	0.17	0.03	0.00	0.11	0.00	0.14
45	$(86.69, 5.39, -5.79)^T$	0.11	0.03	0.00	0.09	0.00	0.08

Table 3
Ply stressed extracted from the FE model, corresponding efforts. From top to bottom ply, $r_{max} = 1.498$.

Ply	$(\sigma_1, \sigma_2, \tau_{12})^T$ in MPa	Eff	$Eff^{\parallel\sigma}$	$Eff^{\parallel\tau}$	$Eff^{\perp\sigma}$	$Eff^{\perp\tau}$	$Eff^{\perp\parallel}$
45	$(307.19, 22.37, -59.11)^T$	0.87	0.09	0.00	0.36	0.00	0.84
−45	$(298.90, 19.74, 51.91)^T$	0.76	0.09	0.00	0.32	0.00	0.73
90	$(-279.26, 36.75, 0.46)^T$	0.60	0.00	0.17	0.59	0.00	0.01
0	$(688.23, 0.49, -0.24)^T$	0.21	0.21	0.00	0.01	0.00	0.00
0	$(572.79, 1.56, 0.00)^T$	0.18	0.18	0.00	0.03	0.00	0.00
90	$(-101.95, 21.90, -0.24)^T$	0.35	0.00	0.06	0.35	0.00	0.00
−45	$(143.84, 10.52, 15.88)^T$	0.25	0.04	0.00	0.17	0.00	0.22
45	$(129.86, 8.07, -8.67)^T$	0.16	0.04	0.00	0.13	0.00	0.12

[1] Note that the following equations intentionally provide multiple digits, in order to avoid unwanted rounding effects, when accuracy is assessed. The technical relevance of the third, fourth or fifth is limited. They can be skipped, once the accuracy has been outlined.

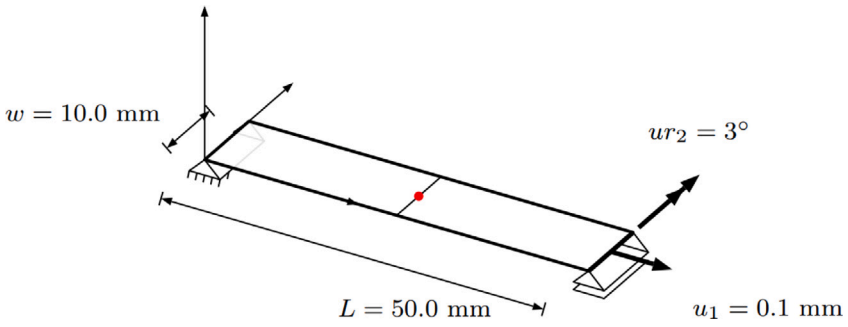

Fig. 9. Example analysis case, with extension loading u_1 and rotation ur_2.

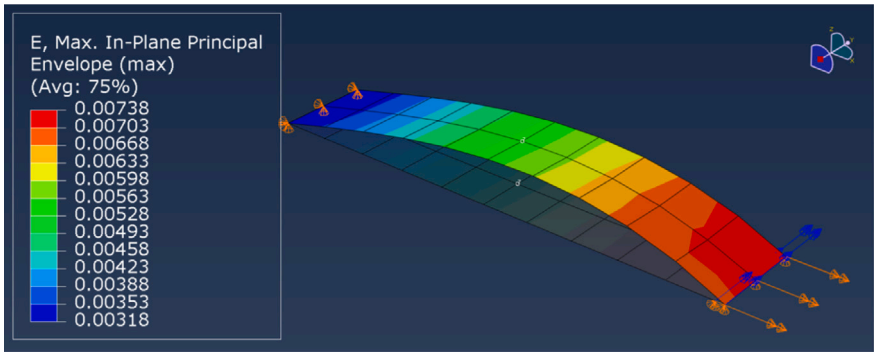

Fig. 10. FE model in ABAQUS. Limit-Load case illustrated. Center location evaluated. Note, that the (Avg:75%) in the figure above refers to an ABAQUS internal visualization setting.

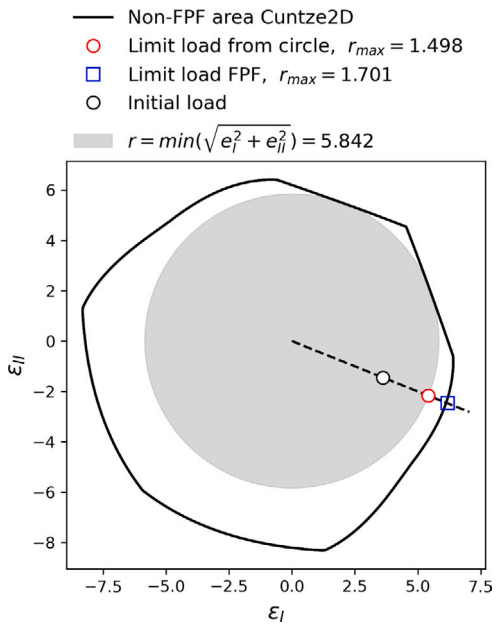

Fig. 11. Results of the use-case application. IM7/977-3, strain in text‰.

use case at hand, a scaling factor of 1.701 is found[2]. It induces the onset of failure of the uppermost 45° ply in the laminate. Corresponding ply stresses, total efforts and mode-specific efforts are given in Table 4.

[2] Note, that the described procedure inherently assumes proportional loading and linear elasticity, which is mandatory for strain ∝ load.

Table 4
Ply stressed extracted from the FE model, corresponding efforts. From top to bottom ply, $r_{max} = 1.701$.

Ply	$(\sigma_1, \sigma_2, \tau_{12})^T$ in MPa	Eff	$Eff^{\parallel\sigma}$	$Eff^{\parallel\tau}$	$Eff^{\perp\sigma}$	$Eff^{\perp\tau}$	$Eff^{\perp\parallel}$
45	$(350.28, 25.50, -67.40)^T$	1.00	0.11	0.00	0.41	0.00	0.96
−45	$(340.82, 22.51, 59.19)^T$	0.87	0.10	0.00	0.36	0.00	0.84
90	$(-318.42, 41.90, 0.53)^T$	0.68	0.00	0.20	0.68	0.00	0.01
0	$(784.75, 0.56, -0.27)^T$	0.24	0.24	0.00	0.01	0.00	0.00
0	$(653.13, 1.78, 0.00)^T$	0.20	0.20	0.00	0.03	0.00	0.00
90	$(-116.25, 24.97, -0.27)^T$	0.40	0.00	0.07	0.40	0.00	0.00
−45	$(164.01, 11.99, 18.11)^T$	0.29	0.05	0.00	0.19	0.00	0.25
45	$(148.08, 9.21, -9.89)^T$	0.19	0.05	0.00	0.15	0.00	0.14

The presented example allows to demonstrate the inherent nonlinearity of the Cuntze FMC. The initial load led to $Eff = 0.57$ (see Table 2). Determining a reserve factor, by inverting this initial effort Eff would have led to $1/0.57 = 1.754$. The incrementally determined FPF-envelope limit is found to be lower, with 1.701. This deviation is a consequence of the formulation of the FMC, mainly due to the exponent parameter m and the mode-specific effort $Eff^{\perp\parallel}$, which scales nonlinearly when a load state is scaled proportionally.

5.1. An alternative approach for directly determining the limit-strain state

An alternative strategy can be pursued to directly determine the limit strain state based on the omni FPF data. When following the usual convention for the principal strain calculation, with $\varepsilon_I > \varepsilon_{II}$, one can define two relevant sectors in the principal strain plot. Those, are defined as:

Each load state can be plotted as a dot, as shown above in Fig. 11. The initial load case for the example at hand (see Eq. (28)) can be attributed to Sector 2. Its angular location can be determined based on ε_I and ε_{II}. The α_ε refers to a triangle, as Fig. 12 shows. The angle is determined to $\alpha_\varepsilon^{ini} = \arctan\left(\frac{|-1.44672|}{3.61965}\right) \approx 21.8°$. The concept for

Table 5
Sector definition for the principal-strain plot.

Sector	ε_I	ε_{II}	α_ε
1	>0	>0	$=\arctan\left(\frac{\varepsilon_{II}}{\varepsilon_I}\right)$
2	>0	<0	$=\arctan\left(\frac{\lvert\varepsilon_{II}\rvert}{\varepsilon_I}\right)$

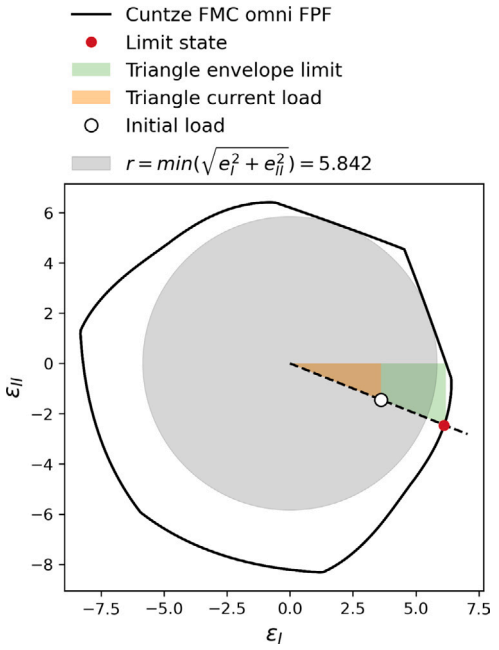

Fig. 12. Using the angle α_ε for direct determining the limit strain state from the envelope data.

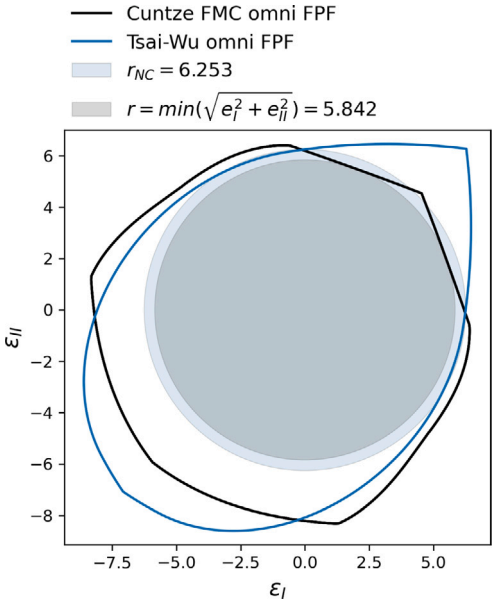

Fig. 13. Tsai–Wu and Cuntze omni envelopes with NC and inner circle; Material: IM7/977-3 from Table 1.

identifying the limit strain state, is to find the point on the envelope, which is positioned on a straight line with the origin and the initial-load point (as in the intercept theorem). In a simple loop, all determined envelope data points in Sector 2 are examined and the corresponding angles $(\alpha_\varepsilon)_i$ are calculated, according to the α_ε definition in Table 5. The point of interest is found by identifying the ith point, which refers to $min(|\alpha_\varepsilon^{ini} - (\alpha_\varepsilon)_i|)$. For the case at hand, the complete envelope consists of 762 points. 180 points are attributed to Sector 2. The best match was found for the point

$$\begin{bmatrix} \varepsilon_I \\ \varepsilon_{II} \\ 0 \end{bmatrix} = \begin{bmatrix} 6.1185 \\ -2.4720 \\ 0 \end{bmatrix} \tag{30}$$

with refers to an angular position of $\alpha_\varepsilon = 22.0°$. The corresponding principal-strain-vector magnitude is determined to $\sqrt{\varepsilon_I^2 + \varepsilon_{II}^2} = 6599‰$. Thus, the scaling factor is $1.6929 = 6599/3898$ for the α_ε-based approach. The value is close to the incrementally determined scaling factor of 1.701, determined in the previous section. The difference can be explained by the point density of the FPF envelope data. The presented procedure identifies the closest point, which leads to an angle discrepancy of 0.2° for the case at hand. Increasing the number of FPF-envelope data points, or using interpolation techniques, will help to further minimize the discrepancy.

6. Conclusions

Omni first-ply-failure (FPF) envelopes are presented as an valuable tool to assess composite laminate failure in context of FE supported composite design processes. Omni envelopes base on conventional Engineering constants and strength parameters in stress space. In recent literature Omni envelopes are presented for the Tsai–Wu criterion. The present article utilizes Cuntze's Failure-mode-concept for the envelope creation process, for the first time.

The article presents two different strategies for directly determining Omni FPF envelopes and it is outlined, why omni envelopes refer to laminate principal strains.

An omni FPF envelope circumscribes all principal-strain states of a laminate, which can be sustained by plies aligned in all conceivable orientations. As long a principal strain state $(\varepsilon_I, \varepsilon_{II})$ is within the envelope, all plies remain intact. An omni envelope is a conservative criterion, as all conceivable ply orientations are captured, which usually leads to the minimum-area envelope.

The provided simple application example outlines how composite design engineers can use those envelopes in context of laminate-failure assessment. Omni envelopes offer unique illustration opportunities. Those are applied for the example case and it is demonstrated how laminate reserve factors are deduced from the envelope representation.

CRediT authorship contribution statement

Erik Kappel: Writing – review & editing, Writing – original draft, Visualization, Methodology, Investigation, Formal analysis, Conceptualization.

Declaration of competing interest

The authors declare that they have no known competing financial interests or personal relationships that could have appeared to influence the work reported in this paper.

Data availability

No data was used for the research described in the article.

Acknowledgments

The project '101101974 - UP Wing' is supported by the Clean Aviation Joint Undertaking and its members.

Co-funded by the European Union

CLEAN AVIATION

Disclaimer

Funded by the European Union. Views and opinions expressed are however those of the author only and do not necessarily reflect those of the European Union or Clean Aviation Joint Undertaking. Neither the European Union nor the granting authority can be held responsible for them.

Appendix

A.1. Tsai–Wu failure criterion and strength ratio definition

The strength-ratio concept. Linearity is inherently assumed. The envelope limit is defined by:

$$\sigma_1 \cdot \left[\frac{1}{X_T} - \frac{1}{X_C}\right] + \sigma_2 \cdot \left[\frac{1}{Y_T} - \frac{1}{Y_C}\right] + \frac{\sigma_1^2}{X_T X_C} + \frac{\sigma_2^2}{Y_T Y_C} + \frac{\sigma_{12}^2}{S^2} - \frac{\sigma_1 \sigma_2}{\sqrt{X_T X_C Y_T Y_C}} = 1 \quad (31)$$

Finding the limit until the failure condition is fulfilled scales the initial load with the factor R. $\sigma_{max} = R \cdot \sigma_{applied} = R \cdot [\sigma_1, \sigma_2, \sigma_{12}]^T$ The resulting equation is rearranged

$$R^2 \cdot \left(\frac{\sigma_1^2}{X_T X_C} + \frac{\sigma_2^2}{Y_T Y_C} + \frac{\sigma_{12}^2}{S^2} - \frac{\sigma_1 \sigma_2}{\sqrt{X_T X_C Y_T Y_C}}\right) + \\ + R \cdot \left(\sigma_1 \cdot \left[\frac{1}{X_T} - \frac{1}{X_C}\right] + \sigma_2 \cdot \left[\frac{1}{Y_T} - \frac{1}{Y_C}\right]\right) - 1 = 0 \quad (32)$$

and the quadratic function

$$R^2 \cdot a + R \cdot b - 1 = 0 \quad (33)$$

is solved for R

$$R = -\frac{b}{2a} + \sqrt{\left(\frac{b}{2a}\right)^2 + \frac{1}{a}} \quad . \quad (34)$$

Fig. 13 shows a comparison of FPF envelopes, developed with the Tsai–Wu or the Cuntze criterion, for IM7/977-3 material.

A.2. Python code

Listing 1: Python code for strain incrementation

```
#incremenation
inc = 12
#magnitude thresholds
mag = 0.01

#range definitions
exrange = np.linspace(-mag,mag,inc)
eyrange = np.linspace(-mag,mag,inc)
gammaxyrange=np.linspace(-mag,mag,inc)

#loops to assess combinations
for ex in exrange:
    for ey in eyrange:
        for gxy in gammaxyrange:

            #global strain vector
            epsglob = np.array([[ex], [ey], [gxy]])
            ...
```

A.3. Mohr principal-strain circle

$$q = \frac{\varepsilon_1 - \varepsilon_2}{2}, \quad p = \frac{\varepsilon_1 + \varepsilon_2}{2}, \quad R = \sqrt{q^2 + (\gamma_{12}/2)^2}$$

$$\varepsilon_I = p + R = \frac{\varepsilon_1 + \varepsilon_2}{2} + \sqrt{\left(\frac{\varepsilon_1 - \varepsilon_2}{2}\right)^2 + (\gamma_{12}/2)^2} \\ = \frac{1}{2}\left(\varepsilon_1 + \varepsilon_2 + \sqrt{(\varepsilon_1 - \varepsilon_2)^2 + \gamma_{12}^2}\right) \quad (35)$$

$$\varepsilon_{II} = p - R = \frac{\varepsilon_1 + \varepsilon_2}{2} - \sqrt{\left(\frac{\varepsilon_1 - \varepsilon_2}{2}\right)^2 + (\gamma_{12}/2)^2} \\ = \frac{1}{2}\left(\varepsilon_1 + \varepsilon_2 - \sqrt{(\varepsilon_1 - \varepsilon_2)^2 + \gamma_{12}^2}\right) \quad (36)$$

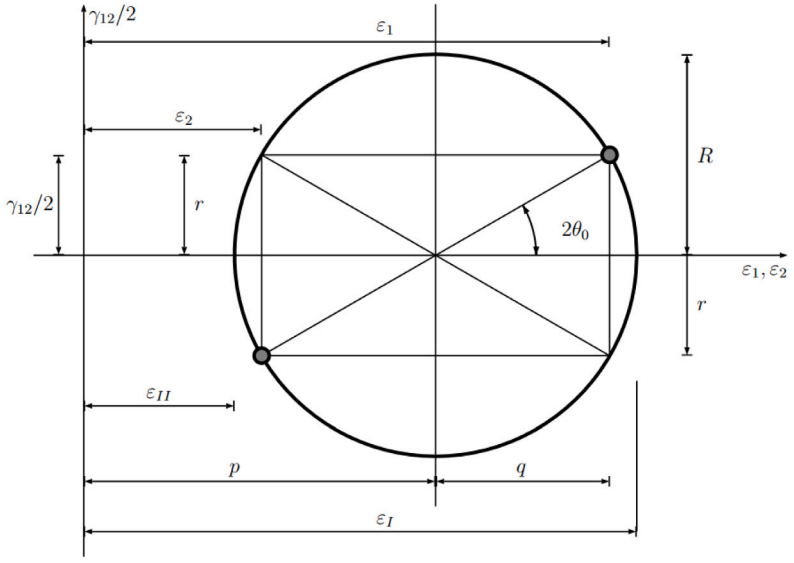

References

[1] S.W. Tsai, J.D.D. Melo, Composite Materials Design and Testing - Unlocking Mystery with Invariants, Stanford University, 2015.

[2] Ralf Cuntze, Life-work cuntze - a compilation, 2022, The Failure-Mode-Concept FMC, a physical and theoretical Material Symmetry-driven basis to generate Strength Criteria, that gave a reason to look after a 'more closed' Strength Mechanics Building & in addition Very Much on Structural Materials, Techniques and Design including work-life experiences of the author in many engineering fields. (about 850 pages), downloadable from https://www.carbon-connected.de/Group/Prof.Ralf.Cuntze.

[3] ABAQUS CAE 6.14-1 manual. Dassault systemes, 2014.

[4] S.W. Tsai, Double-double: New family of composite laminates, AIAA J. (2021) http://dx.doi.org/10.2514/1.J060659.

[5] S.W. Tsai, B.G. Falzon, A. Arav, DOUBLE-DOUBLE Simplifying the Design and Manufacture of Composite Laminates, Composite Design Group, Stanford University, 2023.

[6] R. Cuntze, E. Kappel, Why not designing multi directional laminates with in-plane strength design sheets applying the UD criteria of Tsai–Wu and Cuntze?, in: Mechanics of Composite Materials, Springer, 2024, (submitted for publication).

[7] R. Cuntze, Comparative characterization of four significant UD strength failure criteria (SFC) with focusing a direct use of friction values, use of 'strength' $R_{\perp\perp}$ and 'Proportional Loading', 2023, https://www.carbon-connected.de/Group/Prof.Ralf.Cuntze/Pages/Start/Index/173223.

[8] S.W. Tsai, et al., DOUBLE-DOUBLE a New Perspective in the Manufacture and Design of Composites, JEC/ Stanford publication, ISBN: 978-0-9819143-3-6, 2022.

[9] A.T. Nettles, Basic Mechanics of Laminated Composite Plates - NASA Reference Publication 1351, Technical Report, NASA, 1994.

[10] S.W. Tsai, J.D.D. Melo, A unit circle failure criterion for carbon fiber reinforced polymer composites, Compos. Sci. Technol. 123 (2016) 71–78.

[11] E. Kappel, Double-double laminates for aerospace applications - Finding best laminates for given load sets, Composites C 8 (2022) 100244.

[12] W.E. Guin, A.T. Nettles, A Straightforward Approach To Thickness Tailoring in Composite Structures using Non-Traditional Layups, NASA/T-20210021062 Marshall Space Flight Center, Huntsville, Alabama, 2021.